Publication IV

L. Aaltonen and K. Halonen. 2008. Integrated high-voltage PID controller. In: Proceedings of the 11th International Biennial Baltic Electronics Conference (BEC 2008). Tallinn, Estonia. 6-8 October 2008. Pages 125-126. ISBN 978-1-4244-2060-5.

2008 International Biennial Baltic Electronics Conference (BEC2008)
Tallinn, Estonia, October 6-8, 2008

Integrated High-Voltage PID Controller

L. Aaltonen, K. Halonen

Department of Micro and Nanosciences, Helsinki University of Technology, Espoo, Finland

ABSTRACT: An integrated continuous time PID controller is presented in this paper. Only two operational amplifiers are used for the controller to minimize the power consumption and area, but also to enable complex zeros. A supply voltage up to 12 V is tolerated and, in order to enable tunable properties of the controller, four resistor matrices are used. Measured results of the controller are presented.

1 Introduction

Any type of closed-loop system requires a controller for realization of desired system behaviour and dynamics. A very common type of controller is a PID controller, which combines a proportional controller (P), integrator (I) and differentiator (D). For example in microelectromechanical systems (MEMS) the feedback is commonly utilized for position control [1], [2]. The integrator provides infinite control accuracy at dc, while the PD-part is required to speed up and stabilize the system.

Although digital controllers are common in mixed-mode systems, purely analog designs still exist where, for example, because of area or noise issues, digital controller cannot be used.

This paper presents the design and implementation of a high-voltage continuous time PID controller, in which pole and zero location can be tuned using resistor matrices. The topology used allows complex zeros and requires two operational amplifiers

2 Implemented PID Controller

The schematic of the controller is shown in Fig. 1. The four resistors are implemented as resistors matrices to allow adjustable controller properties. The two capacitors have constant values and integrator capacitor C_3 is left external. The transfer function for the controller can be calculated as

$$H_{PID}(s) = V_{out} / V_{in} = \frac{As^2 + Bs + C}{Ds^2 + s}, \qquad (1)$$

where

$$A = R_2 C_1 (R_x + R_1) / R_1, \qquad (2)$$

$$B = \frac{R_2}{R_1} + \frac{C_1 R_x}{C_3 R_3} + \frac{C_1 R_2 (R_x + R_1)}{C_3 R_3 R_1}, \qquad (3)$$

$$C = (R_2 + R_1) / C_3 R_3 R_1 \qquad (4)$$

and

$$D = R_x C_1 . \qquad (5)$$

The components in the equation correspond to the figure. The supply voltage used for the controller is 12 V and the common mode (CM) voltage of the input V_{in} is the same as the CM voltage of the output V_{out}, which is defined by the reference V_{mid} of 6 V.

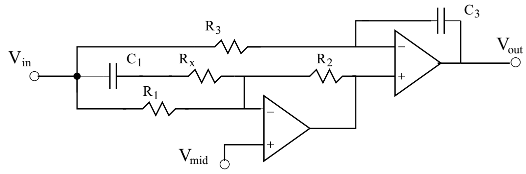

Fig. 1 The topology of the PID controller. The resistors are implemented as controllable matrices with a 4-bit control word for each resistor.

The two operational amplifiers are required to be able to operate with resistive feedback and load of 50 kΩ, while the high-voltage supply sets voltage tolerance requirements for the components. Based on these specifications the two stage amplifier of Fig. 2 is used. The number of high-voltage transistors needed was kept as small as possible to reduce the number of area consuming high-voltage transistors. In addition, the low-voltage transistors provided better matching and, for example, the noise sources were better characterized. The diodes of the schematic protect the low voltage transistors and are in non-conducting state during normal operation. The systematic offset resulting from unequal gate voltages between MN1 and MN3 is below half a millivolt at the amplifier input.

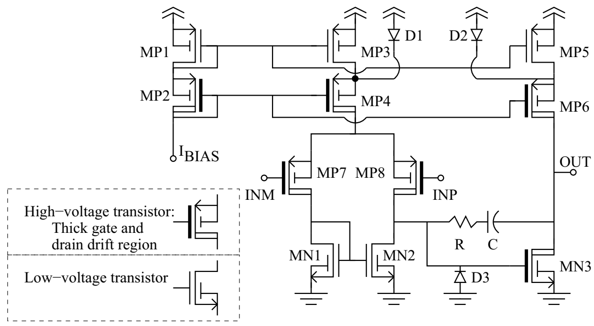

Fig. 2 The operational amplifier used for the controller.

Thin oxide could be used for the high-voltage transistors also because the gate-source voltages are always limited. Hence, the voltage tolerance of the amplifier depends on

978-1-4244-2060-5/08/$25.00 ©2008 IEEE

the drain-source voltage tolerance of the high-voltage transistors. The biasing of cascodes in the amplifier is not optimized and the cascode transistor (MP6) can fall to linear region during normal operation. This is tolerated as even with an output amplitude of 11.6 V peak-to-peak the linearity is still almost 100 dB at 1 kHz.

The resistor matrices require floating switches so that different resistor values can be selected. A traditional floating transmission gate switch cannot be used in case the bulk terminal is tied to the source terminal because the resulting diode between the switch terminals can become forward biased during normal operation. For this reason the switch of Fig. 3 is used. The drain-source diodes of switch transistors (MN1, MN2, MP2, MP1) are connected anti-series and cannot therefore conduct. The minimum sized PMOS transistor MP3 has fairly small cross-coupling decreasing effect. A CMOS structure is used in order to enable use of rail-to-rail signals and the level shifter is needed to provide the differential high-voltage control signals for the switch transistors. It should be notified that the MOSFETs of the switch must tolerate gate-source voltage as high as the high-voltage supply. If only thin oxide is available, the gate control of the switch transistors becomes very complicated as full scale clock signals cannot be used.

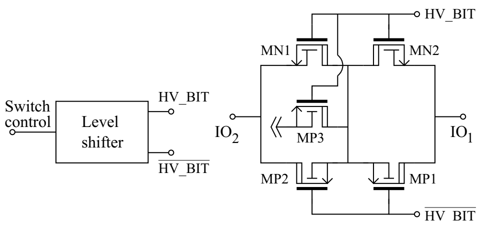

Fig. 3 A floating high-voltage switch, where high-voltage transistors with shorted source-bulk terminals are used.

3 Measured Results

The microphotograph of the implemented chip is shown in Fig. 4. The chip area is 22 mm^2, while the controller area (encircled area in the figure) is 1.8 mm^2. The technology used is a 0.7 µm high-voltage CMOS technology with high-ohmic polysilicon resistors and linear analog capacitors. Most of the controller area is taken by the high-voltage switches. The supply voltage is 12 V, the reference 6 V and the supply current 0.55 mA.

Three different settings were applied for the controller by selecting different resistor values. The corresponding transfer functions were measured using HP 4195A network analyzer. The results are shown in Fig. 5, where (1) is used to calculate the theoretical results. The discrepancy between measured and theoretical phase stems at low frequencies from saturating analyzer and at high frequencies from operational amplifier properties. At high frequencies the second pole of the system limits the gain of the controller. Above this pole, determined by D in (1), the controller gain is frequency independent up to region where the amplifier starts to attenuate the signal.

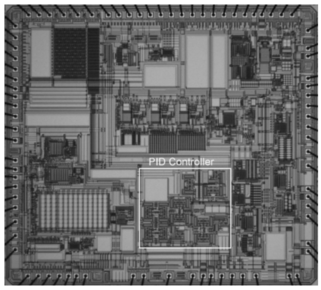

Fig. 4 The microphotograph of the implemented chip.

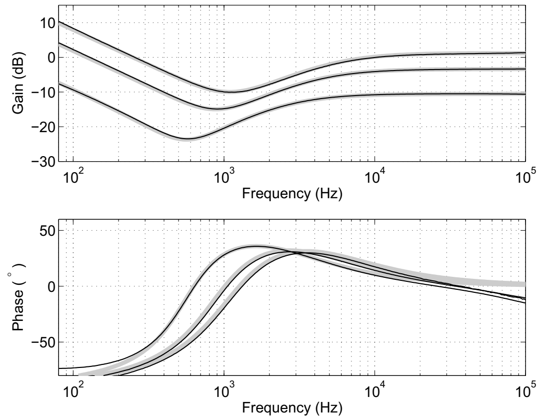

Fig. 5 The measured transfer functions of the controller in three different cases. The black lines correspond to measured and grey ones to theoretical results.

4 Conclusions

An integrated PID controller utilizing two amplifiers and enabling complex zeros is presented. The switches used for components matrices must have gate oxide that tolerates voltages as high as supply, whereas the amplifiers can be implemented using thin oxide high-voltage transistors. The controller chip area is dominated by the high-voltage switches, where the transistors require wide spacing.

Acknowledgement

The authors wish to thank VTI Technologies Oy and Finnish Funding Agency for Technology and Innovation (TEKES) for financial support.

References

[1] L. Wang, J.M. Dawson, L.A. Hornak, P. Famouri and R. Ghaffarian, “Real-time translational control of a MEMS comb resonator”, IEEE Trans. Aerosp. Electron. Syst., vol. 40, no. 2, April 2004, pp. 567-568.

[2] S. Pannu, C. Chang, R.S. Muller, A.P. Pisano, “Closed-loop feedback-control for improved tracking in magnetically actuated micromirrors”, In Proc. IEEE Int. Conf. Optical MEMS, Aug. 2000, pp. 107 – 108.